Plato proposed that, although real objects cannot have all the properties of ideal geometrical objects, certain reflections of ideality should still be present in real objects. Knotted polymeric chains provide an interesting example of a relation between ideal geometrical representations and real physical objects. □

Received 21 May; accepted 2 October 1996.

1. Alexander, J. W. *Trans. Am. Math. Soc.* **30,** 275–306 (1928).
2. Jones, V. F. R. *Bull. Am. Math. Soc.* **12,** 103–111 (1985).
3. Freyd, P. *et al. Bull. Am. Math. Soc.* **12,** 239–246 (1985).
4. Vassiliev, V. A. in *Theory of Singularities and its Applications* (ed. Arnold, V. I.) 23–70 (Am. Math. Sco., Providence, 1990).
5. Stasiak, A., Katritch, V., Bednar, J., Michoud, D. & Dubochet, J. *Nature* **384,** 122 (1996).
6. Moffatt, H. K. *Nature* **347,** 367–369 (1990).
7. Chui. & Moffatt, H. K. *Proc. R. Soc. Lond. A* **451,** 609–629 (1995).
8. Simon, J. in *Mathematical Approaches to Biomolecular Structure and Dynamics* (eds Mesirov, J. P., Schulten, K. & Summers, D. W.) 39–58 Springer, New York, (1996).
9. Grosberg, A., Feigel, A. & Rabin, Y. *Phys. Rev. E* (in the press).
10. Frank-Kamenetskii, M. D., Lukashin, A. V. & Voogodskii, A. V. *Nature* **258,** 398–402 (1975).
11. Vologodskii, A. V., Levene, S. D., Klenin, K. V., Frank-Kamenetskii, M. & Cozzarelli, N. R. *J. Mol. Biol.* **227,** 1224–1243 (1992).
12. Katritch, V. *et al. J. Mol. Biol.* **254,** 591–594 (1995).
13. Frank-Kamenetskii, M. D. & Vologodskii, A. V. *Sov. Phys. Usp.* **24,** 679–696 (1981).
14. Rolfsen, D. *Knots and Links* (Publish or Perish, Berkeley, 1976).
15. Adams, C. C. *The Knot Book* (Freeman, New York, 1994).
16. Fuller, F. B. *Proc. Natl Acad. Sci. USA* **68,** 815–819 (1971).
17. Bednar, J. *et al. J. Mol. Biology* **235,** 825–847 (1994).
18. Rybenkov, V. V., Cozzarelli, N. R. & Vologodskii, A. V. *Proc. Natl Acad. Sci. USA* **90,** 5307–5311 (1993).
19. Metropolis, N., Rosenbluth, A. W., Rosenbluth, M. N., Teller, A. H. & Teller, E. *J. Chem. Phys.* **21,** 1087–1092 (1953).

ACKNOWLEDGEMENTS. This work was supported by the Swiss National Foundation and by Foundation Herbette, University of Lausanne.

CORRESPONDENCE should be addressed to A.S. (e-mail: Andrzej.Stasiak@lau.unil.ch).

Dislocation-mediated melting of a two-dimensional crystal

L. Pauchard, D. Bonn & J. Meunier

Laboratoire de Physique Statistique de l'ENS, URA 1306 du CNRS, associé aux universités Paris VI et Paris VII, 24 rue Lhomond, 75231 Paris cedex 05, France

MELTING of three-dimensional solids usually starts at the free surface, which typically melts at a lower temperature than the bulk material[1]. In two dimensions the starting point of many studies is the Kosterlitz–Thouless theory[2,3], in which melting is initiated through dislocation unbinding. Langmuir monolayers—single layers of amphiphilic molecules formed at the air–water interface—should provide an ideal model for studying melting in two dimensions. Here we show that for monolayer crystals of fatty acids coexisting with their liquid phase, the interior melts before the edges. The melting of crystals under mechanical stress is initiated along the line at which the internal stress vanishes. We suggest that this apparently counterintuitive result arises from defect migration to the region of zero stress, where they accumulate and nucleate melting. These results support the idea that defects play a crucial role in melting of two-dimensional systems.

We prepared two-dimensional crystals by compression of a Langmuir film of pure NBD-stearic acid[4–6] (12-(*N*-methyl)-*N*-((7-nitrobenz-2-oxa-1,3-diazol-4-yl)amino)octadecanoic acid). Rectangular crystals (typically $40 \times 1,000\,\mu m$) nucleate and grow in the two-dimensional liquid phase with which they are in equilibrium. The crystallization transition is strongly first-order: the area per molecule in the liquid phase is three times larger than in the solid phase[4,5]. Moreover, the Young's modulus E of these crystals is 6 ± 2 times the value calculated at the dislocation unbinding transition[6]. Melting of the crystals can be achieved by two different thermodynamic processes (heating and decompression) and by a photochemical process. In the latter process, illumination with blue light (which is strongly absorbed by the crystals) shifts the solid/liquid phase boundary, leading to the melting of the crystal. This occurs through a reversible photochemical reaction with oxygen in the air leading to freezing-point depression. The three processes lead to strictly analogous behaviour, indicating a common mechanism for the initiation of the melting. The melting starts either from the short sides of the crystal or from the inside. The dynamics of melting are very slow and the long sides of the crystal are very difficult to melt, leaving two strips of crystal each 2 μm wide after the bulk has melted completely (Fig. 1). For melting by a heating, a period of ~120 min is necessary to melt the bulk for a temperature increase of 1 °C (30 min for 4 °C) above the equilibrium temperature. On this timescale, the remaining strips melt only after an increase in temperature of ~10 °C. Melting obtained by decreasing the surface pressure (Fig. 1*a*, *b*) or by illumination (Fig. 1*d*) shows identical behaviour. The 2 μm length scale is reproducible from experiment to experiment and is independent of the width of the crystal.

Two new boundaries can be created by breaking the two-dimensional crystal into two pieces along a line roughly parallel to the long sides (Fig. 2*a*). If these pieces of crystal are illuminated just after their creation, the two newly created boundaries and the bulk melt simultaneously. When illuminated more than 20 minutes after the breaking, the two new boundaries do not melt (Fig. 2*b*). During this waiting time, the width of the pieces of crystal is

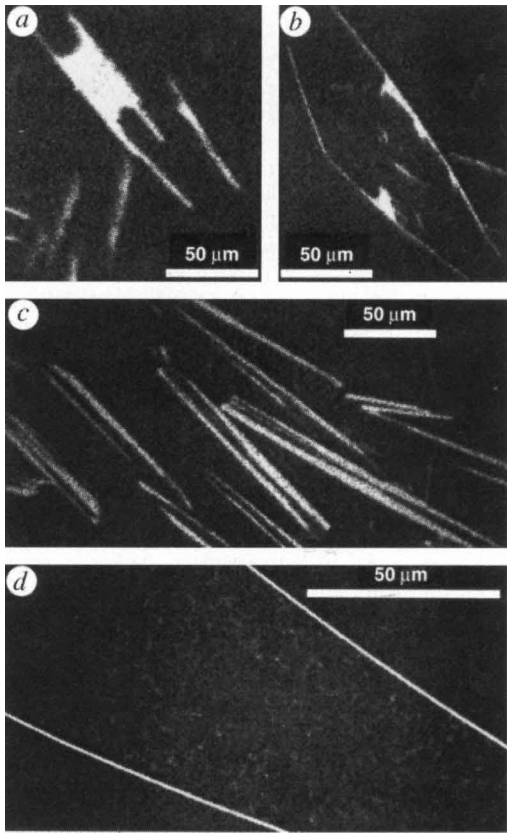

FIG. 1 Fluorescence microscopy images of the NBD-stearic acid system at solid–liquid phase coexistence. In the two-dimensional liquid phase the fluorescence is quenched, whereas the solid domains fluoresce and appear light against a dark background. *a*, Melting obtained by decompression of the rectangular crystals; it starts from the two short sides. In *b*, two strips (one along each long side) resist melting. *c*, Melting obtained by heating; the image was taken 120 min after a temperature increase of 1 °C. *d*, Melting obtained by illumination. The melting occurs everywhere inside the crystal while the strip along each long side does not melt.

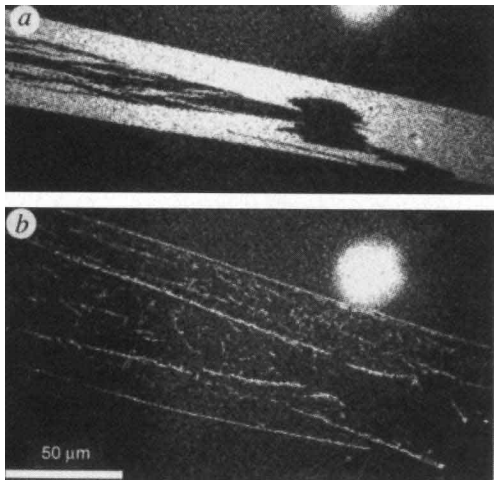

FIG. 2 Breaking and subsequent melting of a two-dimensional crystal. *a*, A small area within the crystal is illuminated until it melts. The increase of surface area upon melting (due to the large difference in area per molecule between the solid and the liquid phase) induces a crack approximately parallel to the long sides of the crystal (because the mechanical properties are anisotropic), creating two new boundaries. *b*, Melting by illumination of the broken crystal 20 min after the breaking. The boundaries along the two long sides of the crystal and the two newly created boundaries do not melt. The bright spot is one of the glass fibres used to immobilize the crystal.

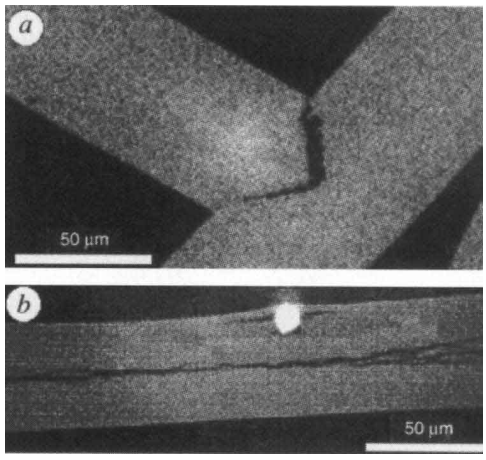

FIG. 3 Local melting by illumination of a crystal. *a*, Rapid melting of a grain boundary between two crystals which were together before illumination. *b*, Melting of a crystal under a bending stress. The melting appears along the neutral line. The bright spot is the image of one of the glass fibres used to bend the crystal. (Two glass fibres immobilize the long ends of the crystal, while a third, mobile, fibre that is apparent on the image is used to apply a force perpendicular to the long axis of the crystal, in its middle. See ref. 6 for details). This fibre has partially penetrated the crystal, inducing a local crack in its vicinity.

constant: the new strips that resist melting result from a change with time of the crystal border. These observations suggest that either the two strips are a different phase, due to a boundary effect, or that the melting nucleates around defects that are expelled from these strips. Order induced by surface effects has been observed in three-dimensional liquid crystals[7], but on length scales much smaller than 2 μm. The long-range dipolar forces that exist in two-dimensional films could explain such long-range effects in our case. However, looking at the polarization of the fluorescence, no difference between the border and the volume can be detected. Also, electron-diffraction experiments[8] repeatedly show only one diffraction pattern. Although the strips along the borders were not specifically looked at in this last experiment, the solid appears to be a single crystal.

The important role of the defects in the initiation of the melting process is revealed by two observations. First, grain boundaries melt much more quickly than the inside of a single crystal (after respectively 5 s and 1 min of illumination under the microscope; Fig. 3*a*). As a grain boundary is an array of dislocations[9], this result indicates that the melting nucleates around defects. A second and very striking observation is that melting by illumination of a two-dimensional crystal under a bending stress (applied with three glass fibres[6]) starts along the neutral line (Fig. 3*b*) where the stress vanishes. From thermodynamics, one expects the contrary to happen: as the stress is released by melting the crystal, the nucleation of the liquid phase should be easier at the points of maximum stress[10]. Surprisingly, melting along the neutral line is also observed when the crystal is illuminated a short time after the stress is relaxed: the crystal has a memory of the stress. However, if we wait for a time $\tau_m \approx 180$ s after the stress release, the crystal melts as if the stress had never been applied. This suggest that melting nucleates around defects that migrate very quickly through the crystal with a diffusion coefficient $D \approx d^2/4\tau_m$, where d is the width of the crystal. This yields $D \approx 10^{-8}\,\mathrm{cm^2\,s^{-1}}$, which may be compared with an estimate for dislocation glide ($D \approx 10^{-6}\,\mathrm{cm^2\,s^{-1}}$) or dislocation climb ($D \approx 10^{-10}\,\mathrm{cm^2\,s^{-1}}$) for two-dimensional crystals[9]. In the stress field, the Peach–Koehler force[11] ($f_p(y) = \sigma b$) causes the dislocations to move ($b = 15 \times 10^{-10}$ m is the Burger vector and $\sigma = Ey/R$ is the stress at a distance y from the neutral line in a bent crystal with radius of curvature R). Depending on their Burgers vector and on the stress field under consideration, the dislocations are advected either to the neutral line or to the crystal border. Under our experimental conditions, the energy of the dislocations advected to the neutral line $\int_0^y f_p(u)\mathrm{d}u$ is large compared to the thermal energy, k_BT, for $y \gtrsim 1$ μm; thus they are rapidly accumulated very close to this line.

Our results imply that, in the absence of external stress, defects must be removed from the crystal edges. This is consistent with fracture experiments on this system[12], in which a delay before breaking was attributed to the spontaneous nucleation of cracks, suggesting that there are no defects at the boundaries. Near the boundary, dislocations interact attractively with their image dislocations (which express mathematically the interaction with the boundary) and so can be removed from the boundary region. However, the large value of E opposes this interaction. Consequently, the large length scale of 2 μm remains a puzzle.

Experiments on melting in three dimensions reveal that superheating of a solid is possible, provided that the liquid phase does not completely wet the solid–gas interface: there is an energy cost for creating the liquid phase bounded by two new interfaces. The main difference from our experiment is that the two-dimensional solid already coexists with its liquid phase. Consequently, line tension effects should not be important for the 'surface melting' of the two-dimensional crystal, as no new line interfaces are created. Together with the observed slowness of the melting of two-dimensional crystals of NBD-stearic acid (but also found for other compounds giving very rigid two-dimensional crystals), this implies a large energetic barrier for the formation of the liquid phase. □

Received 1 July; accepted 8 October 1996.

1. Frenken, J. W. M. & van Pinxteren, H. M. in *The Chemical Physics of Solid Surfaces* Vol. 7 (eds King, D. A. & Woodruff, D. P.) Ch. 7 (Elsevier, Amsterdam, 1994).
2. Kosterlitz, J. M. & Thouless, D. J. *J. Phys. C* **6,** 1181–1203 (1973).
3. Strandburg, K. J. *Rev. Mod. Phys.* **60,** 161–207 (1988).
4. Bercegol, H., Gallet, F., Langevin, D. & Meunier, J. *J. Phys. (France)* **50,** 2277–2289 (1989).
5. Bercegol, H. *J. Phys. Chem.* **96,** 3435–3441 (1992).
6. Bercegol, H. & Meunier, J. *Nature* **356,** 226–228 (1992).
7. Pershan, P. S. & Als-Nielsen, J. *Phys. Rev. Lett.* **52,** 759–762 (1984).

8. Flament, C. *et al. J. Phys. II (France)* **4,** 1021–1032 (1994).
9. Bruinsma, R., Halperin, B. I. & Zippelius, A. *Phys. Rev. B* **25,** 579–582 (1982).
10. Lifschitz, I. M. & Guilida, L. S. *Dokl. Acad. Nauk.* **87,** 377–380 (1952).
11. Peach, M. & Koehler, J. S. *Phys. Rev.* **80,** 436–439 (1950).
12. Pauchard, L. & Meunier, J. *Phys. Rev. Lett.* **70,** 3565–3568 (1993).

ACKNOWLEDGEMENTS. We thank J. Prost, Y. Pomeau and J. Frenken for useful discussions.

CORRESPONDENCE should be addressed to J. M. (e-mail: jmeunier@physique.ens.fr).

Nanotubes as nanoprobes in scanning probe microscopy

Hongjie Dai, Jason H. Hafner, Andrew G. Rinzler, Daniel T. Colbert & Richard E. Smalley

Center for Nanoscale Science and Technology, and Departments of Chemistry and Physics, Rice University, Houston, Texas 77251, USA

SINCE the invention of the scanning tunnelling microscope[1], the value of establishing a physical connection between the macroscopic world and individual nanometre-scale objects has become increasingly evident, both for probing these objects[2–4] and for direct manipulation[5–7] and fabrication[8–10] at the nanometre scale. While good progress has been made in controlling the position of the macroscopic probe of such devices to sub-ångström accuracy, and in designing sensitive detection schemes, less has been done to improve the probe tip itself[4]. Ideally the tip should be as precisely defined as the object under investigation, and should maintain its integrity after repeated use not only in high vacuum but also in air and water. The best tips currently used for scanning probe microscopy do sometimes achieve sub-nanometre resolution, but they seldom survive a 'tip crash' with the surface, and it is rarely clear what the atomic configuration of the tip is during imaging. Here we show that carbon nanotubes[11,12] might constitute well defined tips for scanning probe microscopy. We have attached individual nanotubes several micrometres in length to the silicon cantilevers of conventional atomic force microscopes. Because of their flexibility, the tips are resistant to damage from tip crashes, while their slenderness permits imaging of sharp recesses in surface topography. We have also been able to exploit the electrical conductivity of nanotubes by using them for scanning tunnelling microscopy.

Multiwalled nanotubes (MWNTs) were prepared in the optimized direct-current carbon arc apparatus reported previously[13]. To use a nanotube as a robust probe we bonded it to the side of the tip of a conventional silicon cantilever using a soft acrylic adhesive 1–10 nm thick (Fig. 1). This permits the nanotube to bend away from its connection whenever the tip is inadvertently 'crashed' into a hard surface, and then to snap back to its original straight position when the tip is withdrawn. Effectively the nanotube is then 'spring loaded' much like the side-view mirror of a car.

When used in tapping-mode scanning force microscopy, SFM (where the change in amplitude of an oscillating cantilever driven near its resonant frequency is monitored as the tip taps the surface; the sharp frequency response of high-quality cantilevers make this technique exquisitely sensitive), a carbon nanotube tip such as that shown in Fig. 1 has the unusual advantage that it is both stiff and gentle. It is stiff because there is no bending of the nanotube at all when it encounters a surface at near-normal incidence until the Euler buckling force[14], F_{EULER} is exceeded:

$$F_{EULER} = \pi^2 YI/L^2 \quad (1)$$

where Y is the Young's modulus, I is the stress moment over the cross-section of the nanotube of radius r ($I \approx \pi r^4/4$) and L is the

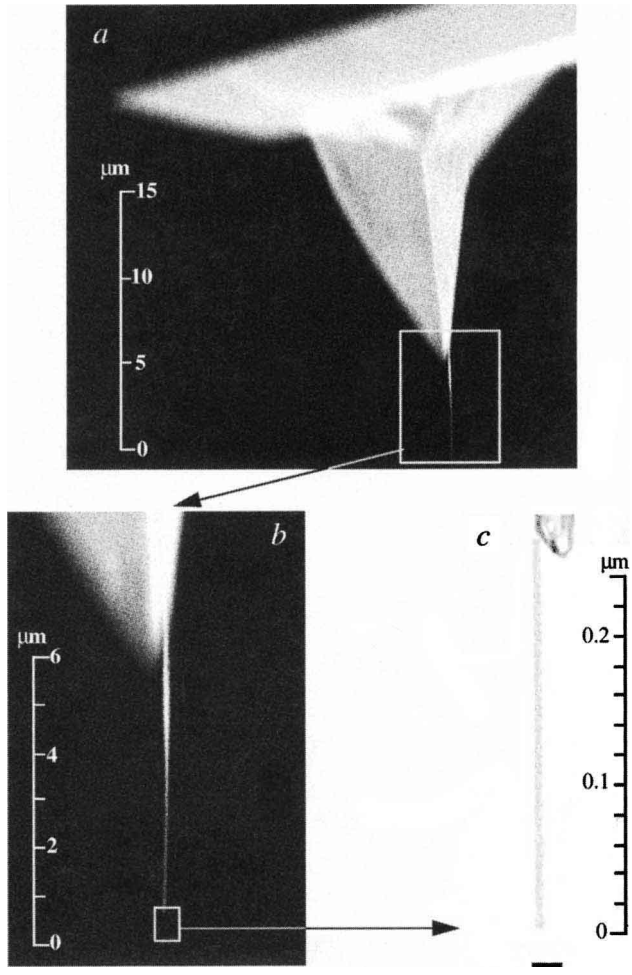

FIG. 1 Single nanotube attached to the pyramidal tip of a silicon cantilever for scanning force microscopy (SFM). The nanotube was attached by first coating the bottom 1–2 μm section of the silicon tip with an acrylic adhesive (by sticking it slightly into an adhesive-coated carbon tape (Electron Microscopy Services, Fort Washington, PA)), and then bringing this tip into contact with the side of a bundle of 5–10 multiwalled carbon nanotubes (MWNTs) while under direct view of an optical microscope using dark-field illumination. Once attached, the nanotube bundle was pulled free from its connections with other nanotubes, leaving a single 5-nm-diameter MWNT extending alone for the final 250 nm. (The most common MWNT diameter obtained at the tip is 5–20 nm, and lengths of single MWNT up to 1 μm are capable of good imaging.) Higher-resolution transmission electron microscopy (TEM) images of this tube showed it to be closed at the tip, as is typical for most MWNTs produced by this arc method (without oxidative etching). *a*, *b*, Scanning electron microscope (SEM) images showing the MWNT bundle attached to the steeper slope of the back side of the silicon pyramid. This attachment ensured that the individual MWNT extending out the end of the bundle, as seen in the TEM image *c*, would approach the surface to be imaged within a few degrees of vertical. Although the adhesive bonding is restricted to within 1–2 μm of the apex, the MWNT bundle continues 5–10 μm further along the side of the pyramid in van der Waals contact. If the pyramid itself is pre-coated with a layer of conductive metal, this method produces a good electrical contact to the MWNT bundle and thereby to the single MWNT probe tip at the end[25]. This attachment method is simple and reliable once the requisite microscope and micro-manipulators are set up. With good-quality MWNT material, mounted probes similar to that shown can be obtained after a few tries. It is useful to have ready access to an electron microscope with a specially-adapted specimen holder to view the cantilever after the MWNT bundle has been attached to see whether the final MWNT at the tip is of the length and diameter desired; after some experience, however, one can simply try imaging with the tips and electro-shortening if necessary. Scale bar in *c*, 20 nm.